Received: 30 June 2018 | Revised: 18 November 2018 | Accepted: 31 December 2018

DOI: 10.1002/ett.3570

SPECIAL ISSUE ARTICLE

WILEY

Regression model for seamless mobility in LTE-A HetNets

A. Saraswathi Priyadharshini | P.T.V. Bhuvaneswari

Department of Electronics Engineering, Madras Institute of Technology, Anna University, Chennai, India

Correspondence
A. Saraswathi Priyadharshini, Department of Electronics Engineering, Madras Institute of Technology, Anna University, Chennai-600 044, India.
Email: ajssara@gmail.com

Abstract

The heterogeneous network (HetNet) deployment in Long-Term Evolution Advanced networks poses serious handover (HO) performance issues when compared to the homogeneous deployment. The solution being the proper configuration of the HO control parameters (HCP), namely, hysteresis margin, A3Offset, cell-specific offset, and TTT in consideration with various characteristics. In the literature, the presented methods rely on either optimization rules or on the unstable network characteristics. The objective of the proposed work is to develop a model for HCP configuration. Initially, sensitivity analysis has been made to investigate the dependency of the abovementioned HCPs with respect to the characteristics, namely, intersite distance and offloading benefit with respect to the HO scenario. Finally, the dependency has been modeled as a regression-based prediction model. Model with the highest prediction accuracy is identified based on the goodness of fit metrics, namely, R-square, adjusted R-square, the sum of square errors, and root-mean-square error, respectively. Among the models explored, the polynomial P44 shows the highest prediction accuracy of 99.29% in macro-pico HO scenario and of 98.61% in pico-macro HO scenario.

1 | INTRODUCTION

Satisfaction of growing user demands and high capacity provision forms the biggest challenge in the upcoming cellular technology.[1] It can be accomplished through cell densification as proven in contemporary cellular networks. In addition, offloading the traffic to provide communication during disaster management can be made through on the spot small cell deployment. The concept of HetNet deployment introduced by 3GPP[2,3] as one of the technical enhancements in LTE-A network plays a vital role in improvising the coverage and capacity of the network. The overlay of small base stations onto the layer of macro base stations is referred as HetNet deployment.[4] An evolved NodeB called eNodeB is the macro base station in LTE-A, which performs the functions of both the NodeB and radio network controller nodes in UMTS.[5] Table 1 presents the lists of acronyms, and Table 2 presents the symbols and definitions.

The small base stations such as microcell, picocell, and femtocell do all the functions of eNodeB but differ in terms of transmitting power it operates on and the ownership, ie, either operator deployed or user deployed. Mobility management in HetNet deployment imposes severe challenges in the perspective of quality-of-service provision. The key element of mobility management is the handover procedure. In general, mobility management is accomplished through an UE assisted and network-controlled hard HO procedure during the connected mode mobility of UE.[6]

However, adopting the same HO procedure impose serious issues such as an increase in HO rate, PP HO rate, and HOF rate when compared to the homogeneous deployment.[7,8] This is due to the facts that (1) disparity in transmit powers of base stations results in varying coverage regions, which initiates more number of HO, (2) high-velocity UE in HetNet

TABLE 1 List of acronyms

Acronyms	Definitions
3GPP	*3rd Generation Partnership Project*
LTE-A	*LTE Advanced*
HetNet	*Heterogeneous network*
eNodeB	*Evolved NodeB*
UMTS	*Universal mobile telecommunications system*
HO	*Handover*
UE	*User equipment*
PP	*Ping-Pong*
HOF	*HO failures*
RLF	*Radio link failure*
MR	*Measurement report*
RSRP	*Reference signal received power*
RSRQ	*Reference signal received quality*
CSO	*Cell-specific offset*
HM	*Hysteresis margin*
A3Off	*A3Offset*
TTT	*Time-to-trigger*
HCP	*HO control parameters*
MP	*Macro-pico*
PM	*Pico-macro*
ISD	*Intersite distance*
MRO	*Mobility robustness optimization*
HOM	*HO margin*
HOS	*HO success*
GoF	*Goodness of fit*
SSE	*Sum of square errors*
RMSE	*Root-mean-square error*

deployment frequently initiates HO, which results in PP HO, and (iii) smaller coverage region of base stations increases the probability of RLF occurrence before the successful completion of HO procedure, which initiates enormous HOF.

The transmission time of MR whether early, on time or late decides the level of HO performance degradation. There are certain control parameters which decide when to transmit the MR. They are defined in the event-based MR reporting criteria of HO procedure.[9] The performance of HO procedure in HetNet can be improved if the control parameters are optimally configured on the basis of certain UE, environmental and network characteristics.

The A3 event-based reporting criterion is predominantly used among the six event-based reporting criteria defined by the 3GPP standard for intraradio access technology HO procedure. It is triggered on the basis of the relative comparison of the received powers rather than on absolute comparisons utilizing thresholds. The A3 event occurs when the RSRP or RSRQ of a target eNodeB becomes greater than the RSRP/RSRQ of a serving eNodeB. The control parameters involved in A3 event are *hysteresis margin (HM), A3Offset (A3Off),* Oc_n (or) Oc_p, Of_n (or) Of_p). Of_n and Of_p (in dB) are the frequency-specific offsets of the target and serving eNodeB. Oc_n and Oc_p (in dB) are the cell-specific offset (CSO) of the target and serving eNodeB. *HM* and *A3Off* (in dB) are the offset parameter for this event, respectively.

To cope with the fading characteristics, the MR is transmitted only whenever the A3event remains active for a duration called time-to-trigger (TTT). In addition, the UE is prevented from transmitting the MR if the A3 event does not get satisfy within that TTT duration. Hence, the control parameters involved in HO procedure initiation are the parameters of A3event (*HM, A3Off,* Oc_n (or) Oc_p, Of_n (or) Of_p) and TTT. The HO performance improvement can be realized when these parameters are properly configured in consideration with factors such as network, UE, and environmental characteristics.

A tremendous amount of work has been done for HCP configuration. The objective of this research is to develop a model for HCP configuration in the HetNet scenario of macro and pico eNodeB deployment. As this work involves the intraradio access technology and intrafrequency HO procedure, the frequency-specific offsets were not considered as both the serving and target eNodeB operate on the same frequency. Hence, the proposed research involves HCPs such as HM,

TABLE 2 Symbols and definitions

Symbols	Definitions
Oc_n and Oc_p	*Neighboring and primary CSO*
Of_n and Of_p	*Neighboring and primary frequency-specific offsets*
S_{eNodeB} and T_{eNodeB}	*Serving and target eNodeB*
(X_M, Y_M)	*Location co-ordinates of macro*
(X_P, Y_P)	*Location coordinates of pico*
(X_i, Y_i)	*Location coordinates of UE*
β_{ISD}	*ISD between S_{eNodeB} and T_{eNodeB}*
α	*Angle of UE movement*
$\mathcal{E}$	*Offloading metric*
β_M and β_P	*Distance from the Macro and Pico eNodeB*
ψ	*Number of HCP combinations*
δ_{MP} (TP)	*Distance at which the A3 event occurs in MP HO scenario*
δ_{PM} (TP)	*Distance at which the A3 event occurs in PM HO scenario*
$\xi_{DL}(\beta_M)$	*Downlink power received at β_M from the macro eNodeB*
$\xi_{DL}(\beta_P)$	*Downlink power received from the pico eNodeB at β_P*
$\mathcal{T}_P$	*Transmitter power*
λ_{TR}	*Path loss between transmitter (T) and receiver (R)*
β_T & β_R	*Antenna gain of T and R*
V_{UE}	*Velocity of UE*
δ_{MP} (TTT) and δ_{PM} (TTT)	*Distance covered by the UE during TTT in MP and PM HO scenarios*
δ_{MP} (MR) and δ_{PM} (MR)	*Distance at which transmission of MR is initiated in MP and PM HO scenarios*
Θ_{PT} & Θ_{ET}	*HO preparation and execution time*
$\delta_{MP}(\Theta_{PT})$ and $\delta_{MP}(\Theta_{ET})$	*Distance traveled by the UE during Θ_{PT} and Θ_{ET}*
$RSRP_{min}$	*Minimum RSRP required by the UE to camp on respective eNodeB*
$RSRP_{RLF}$	*RSRP value which results in RLF*
γ	*Number of HOS groups*
p and q	*Degree of the independent variables*

A3Off, CSO (Oc_n or Oc_p), and TTT. As the HO between pico to pico is very rare, this work focuses only on MP and PM HO scenarios. The control parameters corresponding to the MP HO scenario are HM, A3Off, Oc_n, and TTT while the control parameters corresponding to the PM HO scenario are HM, A3Off, Oc_p, and TTT, respectively.

Initially, the impact of the HCP with respect to the characteristics, namely, ISD and offloading benefit in an urban environment, has been analyzed through sensitivity analysis. Then, the analysis has been extended to study the dependence of these characteristics on HO performance improvement. Finally, a regression-based prediction model has been developed based on the outcome of these analyses for both the HO scenarios.

The organization of this paper is as follows. Section 2 provides a brief review of the related works in the literature. Section 3 explains the system model adopted, the methodology of the proposed analysis, and the development of a regression-based prediction model. The results and discussions of the research carried out are detailed in Section 4. Finally, conclusion and future scope of the work are presented in Section 5.

2 | LITERATURE SURVEY

This section discusses the HCP configuration methods seen in the literature. In the work of Al-Turjman,[10] the importance of small cell deployment in smart grid applications has been presented with respect to the mobility analysis. Lee et al[11] have proposed and investigated the two HCP configuration methods, namely, "adaptive" and "grouping". In the adaptive method, the authors have selected the TTT value with respect to fixed UE speed, whereas in the grouping method, an

optimal TTT value is assigned to the UE speed of a specific range based on RLF rate of 2% and lowest PP rate. The HO performance has also been evaluated with TTT value fixed to 0 ms (case 1), 256 ms (case 2), and 5120 ms (case 3). The simulation results showed the performance with grouping method is as similar to that in the adaptive method. However, significant improvement in HO performance was observed compared to that of the cases with fixed TTT value, irrespective of the target cell-type configurations.

Barbera et al[12] have studied the dependency of the characteristics such as velocity, pico density, type of UE movement (either hot spot/free-moving users) on HO performance. The results predict that drastic increase in HOF, RLF, and PP rate were seen as velocity increases. In addition, the HO rate increases with respect to the density of picocell deployment and it decreases with respect to the hot spot radius. Similar statistics have been observed with free users when hot spot radius is greater than 100 m.

The simulation study presented in the work of Lim and Hong[13] is the extension of the work presented in the work of Lee et al.[11] In addition to the control parameter called TTT, the optimal HM value which results in 2% RLF and lowest ping-pong rate has been identified for each UE velocity and cell-type configuration. From the results, it is seen that the control parameter HM has a high impact of HM in mitigating the PP effect in addition to the TTT value configuration.

The impact of control parameters such as A3Off, CSO, and TTT on HO performance has been analyzed in the work of Mehta et al.[14] The conclusions drawn from the analysis are (1) offloading is limited with a positive value of A3Off and vice versa, (2) during PM HO, configuring the larger value of CSO increases the time of stay in pico, and (3) the value of TTT should be configured considering both the characteristics such as UE velocity and cell-type configuration.

In the work of Kollias et al,[15] the suggestions from the outcome of the simulation analysis are that, to guarantee the improved HO performance, the value of TTT should be selected based on the metrics, namely, ISD and UE velocity. In addition, a high value of TTT is suitable for lesser ISD, whereas for larger ISD, a smaller value of TTT is convenient. The HO performance metrics considered in this analysis are HO, RLF, HOF, and PP rates.

An extensive simulation analysis has been carried out to study the influence of ISD and *angle of UE movement (α)* in the work of Saraswathi Priyadharshini and Bhuvaneswari.[16] The HCPs considered in this analysis are HM, A3Off, and TTT respectively. Furthermore, in the other work of Saraswathi Priyadharshini and Bhuvaneswari,[17] the impact of the HCPs related to HetNet deployment, namely, HM, A3Off, CSO, and TTT, is studied with respect to ISD and α. The conclusions arrived at from the above two analysis are as follows: (1) the HO will trigger early for lesser ISD and vice versa for the same value of the HCP, (2) the HCP value which results in HOS for a smaller value of α induces HOF with a larger value of α, (3) the MP HO should be initiated when the UE is moving closer to the pico eNodeB (approximately $\alpha \leq 10°$), (4) the PM HO can be initiated at a maximum of $\alpha \leq 50°$, and (5) a larger value of bias improves HO performance in the MP HO scenario, whereas smaller bias is appreciable in the PM HO scenario.

In the work of Munoz and Barco,[18] a sensitivity analysis was performed for the two HCPs, namely, CSO and TTT, under different load levels and user velocities. The outcome highlights that the adjustment of TTT provided smaller improvement than the parameter CSO. Thus, an fuzzy logic controller that optimizes CSO was proposed with several sets of manually defined fuzzy rules based on the network and environmental behavior. The proposed method improves the network performance with cell-pair-wide optimization and achieves a good trade-off between call drop rate and HO rate.

Mwanje and Mitschele-Thiel[19] have developed a Q-learning-based MRO algorithm that learns the appropriate value of HM and TTT for the respective UE velocity. It can be inferred from the simulation results that the presented algorithm is able to learn the control parameter values in environments with different velocities.

Hegazy and Nasr[20] have developed an algorithm that optimizes the HCPs, namely, HOM and TTT, based on the performance of different category of UEs. The velocity and traffic type are the metrics used for UE categorization. In each optimization step, the control parameters are configured on the basis of the performance metrics associated with each UE category. The results indicate that the presented method outperforms the existing methods and is ineffective with respect to UE speed.

Becvar and Mach[21] have developed two models to configure the value of HM. The received signal strength indicator was the metric based on which the first model was developed while the other model utilized the metric called carrier to interference plus noise ratio. Both these methods outperform the conventional method, which assigns fixed HM value. Saraswathi Priyadharshini and Bhuvaneswari[22] have developed a regression model from the analysis outcome presented in the other work of Saraswathi Priyadharshini and Bhuvaneswari.[16] The model is based on the metrics, namely, ISD and α. The method presented does not rely on any expert knowledge in framing rules and the fluctuations in the HO performance are avoided. Hence, the developed model improves the HO performance when compared to other methods in the literature.

The conclusion from the findings seen in the literature are that the works[11-17] have made an analysis to study the impact of certain characteristics such as UE velocity, load, and traffic type on HCP configuration. This type of HCP configuration based on the irregular characteristics is highly inefficient as the HO performance oscillates more around the optimal value. In addition, the outcome of these works presents the fact that each HCP has its own significance in HO performance improvement. In addition, the combined impact of all the HCPs was not considered in most of the work. This results in the need to analyze the combined impact of all the HCPs with respect to constant metric thereby HO performance is improved.

The works of Munoz et al,[18] Mwanje and Mitschele-Thiel,[19] and Hegazy and Nasr[20] have presented an optimization algorithm to configure the control parameters. The method of optimization in HCP configuration has drawbacks such as (1) the formulation of optimization rules is rather complicated for a network of stochastic nature and (2) the consideration of irregular characteristics is not appropriate for the long-term stability of the network.

The works of Becvar and Mach[21] and Saraswathi Priyadharshini and Bhuvaneswari[22] present the model-based HCP configuration, which is developed on the basis of metrics such as received signal strength indicator, carrier to interference plus noise ratio, ISD, and α. This method of HCP configuration eliminates the drawback of optimization methods. Hence, sensitivity analysis has been made in this research initiative to study the dependency of ISD and offloading benefit in HetNet deployment. Furthermore, a regression-based prediction model for HCP configuration in HetNet deployment has been developed from the outcome of the analysis.

3 | PROPOSED METHODOLOGY

In this section, the system model considered and the proposed analysis followed by the model development is elaborated. The objective is to develop a regression-based model to configure the HCP on the basis of certain characteristics. A preliminary analysis has been made to study the impact of the characteristics such as β_{ISD} and $\mathcal{E}$ on HO performance and utilized the obtained outcome for the development of a model.

3.1 | System model

The system model considered in the proposed methodology for the MP and PM HO scenarios is presented in Figure 1.

Let "S_{eNodeB}" be the serving eNodeB, "T_{eNodeB}" be the target eNodeB, and "β_{ISD}" be the ISD between them. Let the UE be located at coordinates (X_i, Y_i) and assumed to move in a straight line making an angle of "α" with respect to the line of "β_{ISD}," where $\alpha = 0°$ represents the straight line movement of UE toward T_{eNodeB}. In the MP HO scenario, let macro eNodeB be S_{eNodeB} and pico eNodeB be T_{eNodeB}. Let pico eNodeB be S_{eNodeB} and macro eNodeB be T_{eNodeB} in the PM HO scenario. The UE is assumed to travel from the S_{eNodeB} and toward the T_{eNodeB} in straight lines at constant velocity and angle but generates no user plane traffic. The typical vehicular UEs have the straight line mobility pattern which, are of particular interest. At any instant, the UE is considered to be at distance $'\beta_M'$ from the macro eNodeB and $'\beta_P'$ from the

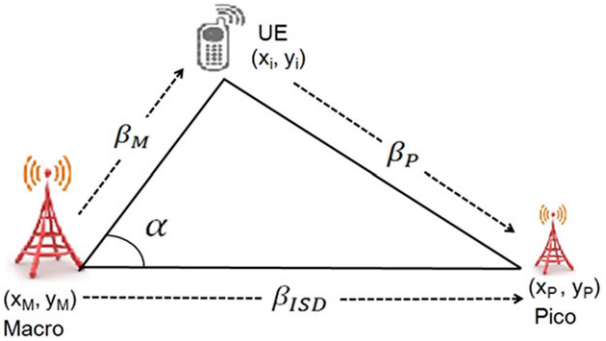

FIGURE 1 System model. HO, handover; MP, macro-pico; PM, pico-macro; UE, user equipment

pico eNodeB. The values of β_M and β_P are computed using the following equation and are represented in kilometer:

$$\beta_M = \sqrt{(X_i - X_M)^2 + (Y_i - Y_M)^2} \tag{1}$$

$$\beta_P = \sqrt{(X_i - X_P)^2 + (Y_i - Y_P)^2}, \tag{2}$$

where (X_M, Y_M) and (X_P, Y_P) are the location coordinates of macro eNodeB and pico eNodeB.

3.2 | Modeling of HO procedure

The HO procedure is modelled in three stages, namely, (1) A3 event occurrence, (2) A3 event persistence, and (3) HO procedure completion. The triggered HO is defined successful if the abovementioned procedure gets completed in a successful manner. They are detailed below.

3.2.1 | Evaluation of A3 event occurrence

Let "δ_{MP} (TP)" and "δ_{PM} (TP)" be the distances at which the A3 event occurs when the UE moves from S_{eNodeB} to T_{eNodeB} in both scenarios of MP and PM HO, respectively. The distance at which A3 event occurs is identified using the following equations:

$$\textbf{\textit{MP HO Scenario}}: \quad \delta_{\mathrm{MP}}(\mathrm{TP}) = \xi_{\mathrm{DL}}(\beta_{\mathrm{P}}) + \mathrm{OC_n} - \mathrm{HM} > \xi_{\mathrm{DL}}(\beta_{\mathrm{M}}) + \mathrm{A3Off} \tag{3}$$

$$\textbf{\textit{PM HO Scenario}}: \quad \delta_{\mathrm{PM}}(\mathrm{TP}) = \xi_{\mathrm{DL}}(\beta_{\mathrm{M}}) - \mathrm{HM} > \xi_{\mathrm{DL}}(\beta_{\mathrm{P}}) + \mathrm{OC_p} + \mathrm{A3Off}, \tag{4}$$

where $'\xi_{\mathrm{DL}}(\beta_M)'$ represents the downlink power received at β_M from the macro eNodeB and $'\xi_{\mathrm{DL}}(\beta_P)'$ is the downlink power received from pico eNodeB at β_P. Both are measured in dBm and are computed using Equation (5)

$$\xi_{\mathrm{DL}}(\beta_M) = \xi_{\mathrm{DL}}(\beta_P) = T_P - \lambda_{TR} + \beta_T + \beta_R \tag{5}$$

where T_P indicates the transmitter power, λ_{TR} the path loss between the transmitter (T), and the receiver (R) and β_T and β_R denote the antenna gain of T and R, respectively.

3.2.2 | Evaluation of A3 event persistence and transmission of MR

Following the occurrence of the A3 event, the persistence of A3 event is verified after the duration of TTT in order to avoid frequent and unnecessary HO. The value of TTT is selected on the basis of the velocity of the UE (V_{UE}) in such a way that the maximum velocity takes a smaller value of TTT and vice versa.[15] Let $'\delta_{\mathrm{MP}}$ (TTT)' and $'\delta_{\mathrm{PM}}$ (TTT)' be the distances covered by the UE for the duration of TTT with respect to the HO scenario. It is computed as follows:

$$\delta_{\mathrm{MP}}(\mathrm{TTT}) = \delta_{\mathrm{PM}}(\mathrm{TTT}) = \frac{\mathrm{V_{UE}}}{TTT}. \tag{6}$$

The transmission of MR is initiated toward the S_{eNodeB} by the UE if the A3 event persists over the distance δ_{MP} (TTT) for the MP HO scenario while it is over the distance δ_{PM} (TTT) for the PM HO scenario. Let $'\delta_{\mathrm{MP}}$ (MR)' and $'\delta_{\mathrm{PM}}$ (MR)' be the distances at which transmission of MR is initiated with respect to the type of the HO scenario. It depends on both δ_{MP} (TP) and δ_{MP} (TTT) for the MP HO scenario and δ_{PM} (TP) and δ_{PM} (TTT) for the PM HO scenario as mentioned in Equations (7) and (8).

$$\textbf{\textit{MP HO Scenario}}: \quad \delta_{\mathrm{MP}}(\mathrm{MR}) = \delta_{\mathrm{MP}}(\mathrm{TP}) + \delta_{\mathrm{MP}}(\mathrm{TTT}) \tag{7}$$

$$\textbf{\textit{PM HO Scenario}}: \quad \delta_{\mathrm{PM}}(\mathrm{MR}) = \delta_{\mathrm{PM}}(\mathrm{TP}) + \delta_{\mathrm{PM}}(\mathrm{TTT}) \tag{8}$$

Once the transmission of MR is initiated, the preparation and execution procedure is to be completed for making the HO procedure successful. Hence, in the next stage, the success of these procedures is verified along with the necessary conditions to be held.

3.2.3 | Evaluation of HO procedure completion

Let " $\delta_{MP}(\Theta_{PT})$ " and " $\delta_{MP}(\Theta_{ET})$ " denote the distances traveled by the UE during HO preparation time (Θ_{PT}) and HO execution time (Θ_{ET}). Let $'\xi_{ULS}'$ be the uplink received power with respect to S_{eNodeB} at the distance δ_{MP} (MR), "ξ_{DLS}" be the downlink received power with respect to S_{eNodeB} at the distance $(\delta_{MP}(MR) + \delta_{MP}(\Theta_{PT}))$, and $'\xi_{ULT}'$ be the uplink received power with respect to T_{eNodeB} at the distance $(\delta_{MP}(MR) + \delta_{MP}(\Theta_{PT}) + \delta_{MP}(\Theta_{ET}))$. Let '$RSRP_{min}$' be the minimum RSRP required by the UE to obtain service from the respective eNodeB and let $RSRP_{RLF}$ represent the RSRP value which results in RLF. Upon receipt of the MR, the S_{eNodeB} triggers the HO to the respective T_{eNodeB}.

The HO procedure is declared to be successfully completed when the following three conditions are satisfied: (1) successful reception of UE-generated MR by S_{eNodeB} at δ_{MP} (MR), which is possible when ξ_{ULS} is greater than or equal to $RSRP_{min}$ as mentioned in Equation (9), (2) ξ_{DLS} should be greater than $RSRP_{RLF}$ for the successful reception of the HO command message by the UE after θ_{PT} as in Equation (10), and (3) as presented in Equation (11), ξ_{ULT} needs to be greater than or equal to $RSRP_{min}$ so that radio link is assumed to be persistent with T_{eNodeB} after θ_{ET}

$$\xi_{ULS}\,(\delta_{MP}\,(MR)) \geq RSRP_{min} \tag{9}$$

$$\xi_{DLS}(\delta_{MP}(MR) + \delta_{MP}(\Theta_{PT})) \;>\; RSRP_{RLF} \tag{10}$$

$$\xi_{ULT}(\delta_{MP}(MR) + \delta_{MP}(\Theta_{PT}) + \delta_{MP}(\Theta_{ET})) \;\geq\; RSRP_{min} \tag{11}$$

3.3 | Preliminary analysis

The analysis is performed as presented in the algorithm below. Let "ψ" be the number of HCP value combinations formulated in this work. Initially, the simulation scenario is created as depicted in the system model and then the performance of the HCP (HM, A3Off, and CSO) with respect to β_{ISD} and $\mathcal{E}$ are analyzed for both the MP and PM HO scenarios. The satisfaction of the HO procedure is verified at each location of the UE for all the HCP value combinations. A suitable combination that results in HOS is identified for the corresponding scenario. This procedure is extended to all the simulation scenarios considered in the analysis to study the impact on HO performance. Similarly, the PM HO scenario analysis has been carried out. The performance metrics utilized in the analysis are a *number of HOS groups* $(\mathcal{Y})$ and *region of HOS* (R_{HOS}). The analysis metric $'\mathcal{Y}'$ is defined as the number of HCP groups that results in HOS, while the metric $'R_{HOS}'$ defines the percentage of the total region to which the HO initiated by the particular HCP group results in success

$$R_{HOS} = \frac{HOS_G}{NL_{Total}} * 100, \tag{12}$$

where $'HOS_G'$ represents the number of locations that results in HOS for the configured group $'G'$, it varies from 1 to $\mathcal{Y}$, and $'NL_{Total}'$ represents the total number of locations considered for triggering the HO. These metrics are applicable to both the MP and PM HO scenarios.

3.4 | Model development

Literature shows that, among the dependent factors, namely, α, β_{ISD}, and $\mathcal{E}$, the probable value of α for the MP HO scenario has to be from 0° to 10°, whereas for the PM HO scenario, it is in the range from 0° to 50°.[17] Hence, the regression-based prediction model needs to be developed on the basis of the dependence of the system characteristics such as β_{ISD} and $\mathcal{E}$ on HCP configuration.

Algorithm 1 Analysis Procedure

1: Initialize i and ψ,
2: Deployment scenario simulation as per system model with specific (β_{ISD} and $\mathcal{E}$)
3: Case 1: MP HO Scenario($\alpha = 0$ to10°)
Configure ($HM(i)$, $A3Off(i)$, $Oc_n(i)$)
if $M_n + Oc_n(i)$ -$HM(i) > M_p + A3Off(i)$, then
if the A3 event persists for the duration of TTT
Verify HO procedure completion
if HOS is accomplished
categorize ($HM(i)$, $A30ff(i)$, $Oc_n(i)$) as HOS group
else
Increment i and repeat from step 3 until (i ≤ ψ)
endif
else
Increment i and repeat from step 3 until (i ≤ ψ)
endif
else
Increment i and repeat from step 3 until (i ≤ ψ)
endif
4: Case 2: PM HO Scenario: ($\alpha = 0$ to 50°)
Configure ($HM(i)$, $A30ff(i)$,$Oc_p(i)$)
if $M_n - HM(i) > M_p + Oc_p(i) + A30ff(i)$, then
if the A3 event persists for the duration of TTT
Verify HO procedure completion
if HOS is accomplished
Categorize ($HM(i)$, $A30ff(i)$, Oc_p(i)) as HOS group
else
Increment i and repeat from step 4 until (i ≤ ψ)
endif
else
Increment i and repeat from step 4 until (i ≤ ψ)
endif
else
Increment i and repeat from step 4 until (i ≤ ψ)
endif
5: Repeat the process from step 2 for all (β_{ISD}, $\mathcal{E}$) combination scenarios.
6: End

For the regression model, the independent variables are β_{ISD} and $\mathcal{E}$. The dependent variable of the model is $'\mathcal{Y}'$, which represents the number of HOS groups that can be configured for a particular simulation scenario. Let us consider the degree of the independent variables β_{ISD} to be $'p'$ and $\mathcal{E}$ to be $'q'$. Equation (13) represents the regression model with a degree of both the independent variables to be one ($p = q = 1$)

$$\mathcal{Y} = \varphi_1 + \varphi_2 \beta_{ISD} + \varphi_3 \mathcal{E} \tag{13}$$

where φ_1, φ_2, and φ_3 are the unknown coefficients. The matrix form of the above linear model is expressed in Equation (14). Let $'m'$ represent the number of unknown coefficients that depend on the degree of the independent variables and let $'n'$ represent the number of simulation scenarios considered

$$\mathcal{Y}^{pq}_{n\,x\,1} = P^{pq}_{n\,x\,m} * \varphi^{pq}_{m\,x\,1} \tag{14}$$

where $p = q = 1$, $'\gamma^{pq}_{n\times 1}'$ is the $(n \times 1)$ matrix representing the number of HOS groups identified for $'n'$ number of simulation scenarios, $'\varphi^{pq}_{m\times 1}'$ is the $(m \times 1)$ matrix indicating the unknown coefficients, and $'P^{pq}_{n\times m}'$ is the design matrix for the regression model. The following equation presents the expanded forms of each of the metric in Equation (14) for the degree p = q = 1:

$$\gamma^{11}_{\mathrm{n\,x\,1}} = \begin{bmatrix}\gamma_1\\ \vdots\\ \gamma_n\end{bmatrix}, \varphi^{11}_{\mathrm{m\,x\,1}} = \begin{bmatrix}\varphi_1\\ \vdots\\ \varphi_m\end{bmatrix}, P^{11}_{\mathrm{n\,x\,m}} = \begin{bmatrix}1 & \beta_{\mathrm{ISD}(1)} & \mathcal{E}_{(1)}\\ \vdots & \vdots & \vdots\\ 1 & \beta_{\mathrm{ISD}(n)} & \mathcal{E}_{(n)}\end{bmatrix} \tag{15}$$

The values of the unknown coefficients in the regression model with any degree of the independent variables are computed using the following equation:

$$\varphi^{\mathrm{pq}}_{\mathrm{m\,x\,1}} = \left(\left(P^{\mathrm{pq}}_{\mathrm{n\,x\,m}}\right)^{\mathrm{T}} * P^{\mathrm{pq}}_{\mathrm{n\,x\,m}}\right)^{-1} * \left(\left(P^{\mathrm{pq}}_{\mathrm{n\,x\,m}}\right)^{\mathrm{T}} * \gamma^{\mathrm{pq}}_{\mathrm{n\,x\,1}}\right) \tag{16}$$

The prediction accuracy of the developed model is identified on the basis of "GoF" statistics. The various performance metrics considered are *SSE, R-square, adjusted-R-square (ARS)*, and *RMSE*.[23]

4 | RESULTS AND DISCUSSIONS

This section discusses the results of the sensitivity analysis and discusses the developed model. The proposed work is simulated using the MATLAB R2014a and the simulation values are adopted as per 3GPP specification. This section presents the preliminary analysis made to identify the dependency between the metrics β_{ISD} and $\mathcal{E}$ on HO performance. The regression model has been developed for both the MP and PM HO scenarios from the outcome of the analysis as presented in Section 4.6. The simulation scenario adopted is presented in Figure 1 and the list of simulation parameters along with the configured values are presented in Table 3.

Analysis has been made for a high-speed UE, taking into account the fact that the combination of HCP values which results in HOS for high speed UE will be highly suitable for low speed UE as well. In the MP HO scenario, the value of α

TABLE 3 Simulation parameters

Parameter	Configured Value
Transmitter power	Macro eNodeB = 46 dBm, Pico eNodeB = 30 dBm, and UE = 23 dBm
Propagation model	Macro to UE = 128.31+ 37.06 ($\log_{10}$(R)), "R" in kilometer[24] Pico to UE = 140.1+ 36.7 ($\log_{10}$(R)), "R" in kilometer[24]
A3 event model	HM = 0 to 15 dB, A3Off = −15 to 15 dB, and CSO = 0 to 16 dB[9]
HO model	Hard HO TTT = 40 ms[13] Preparation delay = 50 ms[24] Execution delay = 40 ms[24]
Velocity of UE (V_{UE})	Urban = Up to 110 km/h
Mobility model	Straight line mobility at constant V_{UE} and α (vehicular UE)
Radio Link Failure ($RSRP_{RLF}$)	−130 dBm
Minimum required RSRP ($RSRP_{min}$)	−110 dBm (3GPP TS 36.301) (to camp on respective eNodeB)
Antenna height	eNodeB = 15 m and UE = 1.5 m[25]
Antenna gain after cable loss	Macro eNodeB (μ_{MT}) = 15 dBi and Pico eNodeB (μ_{PT}) = 8 dBi
Antenna pattern	Omnidirectional
Carrier frequency	2.0 GHz[25]

TABLE 4 Groups with the same δ_{MP} (MR) and δ_{PM} (MR)

Group	(HM, A3Off, CSO) in dB
G1	(0, −15, Oc_n/Oc_p)
G2	(5, −15, Oc_n/Oc_p) (0, −10, Oc_n/Oc_p)
G3	(10, −15, Oc_n/Oc_p),(5, −10, Oc_n/Oc_p) (0, −5, Oc_n/Oc_p)
G4	(15, −15, Oc_n/Oc_p),(10, −10,Oc_n/Oc_p),(5, −5,Oc_n/Oc_p) (0, 0, Oc_n/Oc_p)
G5	(15, −10,Oc_n/Oc_p),(10, −5,Oc_n/Oc_p),(5, 0, Oc_n/Oc_p) (0, 5, Oc_n/Oc_p)
G6	(15, −5,Oc_n/Oc_p),(10, 0, Oc_n/Oc_p),(5, 5, Oc_n/Oc_p) (0, 10, Oc_n/Oc_p)
G7	(15, 0, Oc_n/Oc_p),(0, 15, Oc_n/Oc_p),(10, 5, Oc_n/Oc_p) (5, 10, Oc_n/Oc_p)
G8	(5,15,Oc_n/Oc_p) (10, 10, Oc_n/Oc_p) (15, 5, Oc_n/Oc_p)
G9	(15, 10, Oc_n/Oc_p) (10, 15, Oc_n/Oc_p)
G10	(15, 15, Oc_n/Oc_p)

is restricted up to 10°, whereas it is up to 50° for the PM HO scenario.[17] The simulation scenario with different values of β_{ISD}, such as 100, 300, 500, 700, 900, and 1100 m, has been considered.

As mentioned in the previous section, the HCPs for the MP HO scenario are *HM, A3Off*, OC_p, and TTT, whereas for the PM HO scenario, the HCPs are *HM, A3Off,* OC_n, and TTT, respectively. The value of TTT has been fixed as 40 ms for the high speed UE.[12] The values of *HM, A3Off,* OC_n, and OC_p considered in this analysis are $HM = \{0, 5, 10, 15\ dB\}$, $A3Off = \{-15, -10, -5, 0, 5, 10, 15\ dB\}$, and $CSO = OC_n = OC_p = \{0, 4, 8, 12, 16\ dB\}$. They result in $\psi = 140$ (=4(HM values)×7(A3Off values)×1(TTT value))×5(CSO value)) combinations of HCP values in this research.

The offloading scenario of $\mathcal{E}$ = null offloading, 25% offloading, 50% offloading, 75% offloading, and 100% offloading results in a set of 30 (=6(β_{ISD} values)×5($\mathcal{E}$ values)) simulation scenarios. All the 140 combinations of HCP values are configured for each simulation scenario to identify the HCP which results in HOS. Hence, there were 4200 (=28 × 30) simulation runs made to study the sensitivity of the parameters with respect to the scenario.

This simulation is made for both the MP and PM HO scenarios which results in 8400 (=2 × 4200) simulation runs in total. The occurrence of the A3 event is verified for all these combinations at consecutive coordinates (X_i, Y_i) during the movement of the UE with respect to S_{eNodeB}. The HCP value combination that results in the occurrence of the A3 event at the same δ_{MP} (TP) and δ_{PM} (TP) distance is grouped under one category. Thus, there are 50(=$\mathcal{Y}$) such groups and it is further categorized as groups from G1 to G10 for each CSO as shown in Table 4.

4.1 | Sensitivity analysis of MP HO scenario

This section presents the sensitivity analysis of the MP HO scenario performed on both the factors considered. Initially, the influence of β_{ISD} on R_{HOS} is analyzed and is followed by the influence of $\mathcal{E}$ on R_{HOS} analysis.

The influence of β_{ISD} on R_{HOS} with null offloading is presented in Figure 2A-F. The observation from the analysis is that 30% is the maximum of R_{HOS} obtained for β_{ISD} of up to 500 m with HCP of early triggering values. In addition, a further decrease in R_{HOS} is observed with increases in β_{ISD}. It is 8.57% for β_{ISD} = 700 m with positive values of HCP and is null with other HCPs and β_{ISD} greater than 700 m. This is due to two reasons: (1) the transmit power disparity exists between S_{eNodeB} and T_{eNodeB} and (2) the possibility of HOF is high as the UE moves away from S_{eNodeB}. Hence, it can be concluded that the maximum possible value of β_{ISD} is 500 m and the success of HO is highly sensitive to β_{ISD}. The analysis is further extended to a study of the impact of $\mathcal{E}$ on R_{HOS}.

Figure 3A-E illustrates the influence of $\mathcal{E}$ on R_{HOS} with β_{ISD} assumed to be 500 m. The results predict that the value of R_{HOS} increases with increase in $\mathcal{E}$. When HCP values which trigger early HO are configures, a maximum of 54% of R_{HOS} is achieved for maximum offloading while it is 28% for null offloading. It is due to the fact that increased value of offloading makes T_{eNodeB} more preferable which in turn triggers the HO early and it results in HOS. Forcible HO occurs in a very early stage with a larger value of $\mathcal{E}$ and vice versa. It shows the dependence on the offloading criteria as well.

In summary, the outcome reveals that the combinations of HCP values which trigger the HO early result in an increased R_{HOS} and vice versa. Thus, the dependence of HO performance on β_{ISD} and $\mathcal{E}$ in the MP HO scenario is identified and they can be used as a potential prediction metric to develop a regression model for optimal HCP configuration.

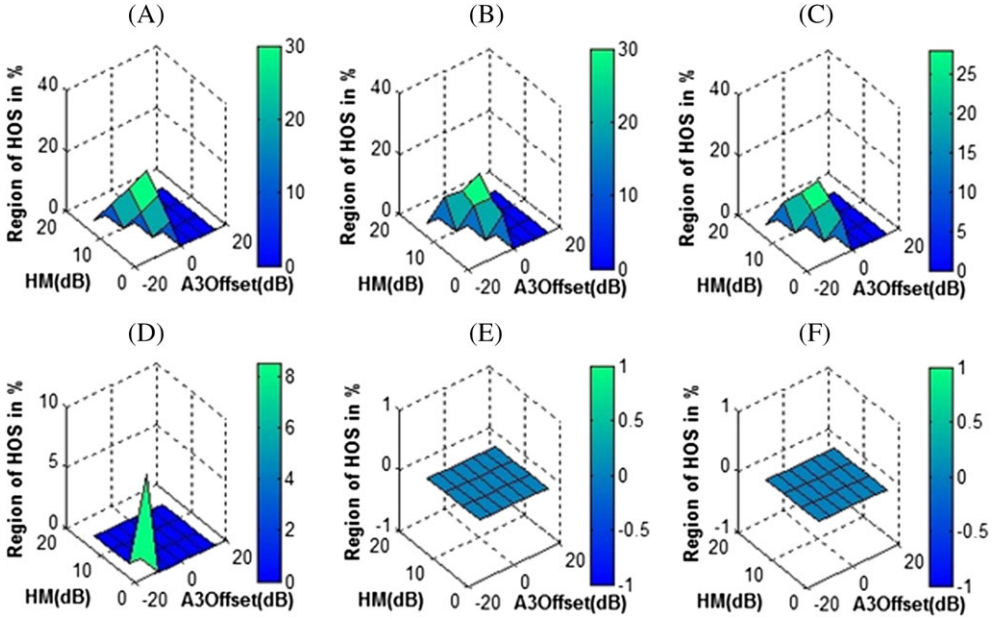

FIGURE 2 Sensitivity analysis of β_{ISD}. A, Macro-Pico ISD = 100m; B, Macro-Pico ISD = 300m; C, Macro-Pico ISD = 500m; D, Macro-Pico ISD = 700m; E, Macro-Pico ISD = 900m; F, Macro-Pico ISD = 1100m

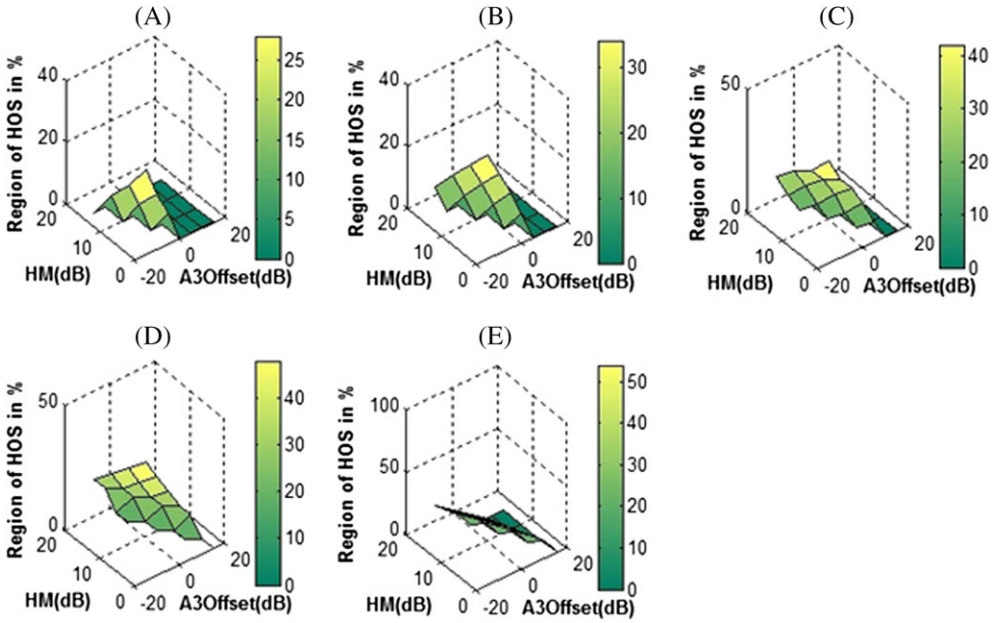

FIGURE 3 Sensitivity Analysis of $\mathcal{E}$. A, CSO = 0 dB; B, CSO = 4 dB; C, CSO = 8 dB; D, CSO = 12 dB; E, CSO = 16 dB

4.2 | Sensitivity analysis of PM HO scenario

Similar to the sensitivity analysis presented in the previous section, the influence of β_{ISD} on R_{HOS} is studied for the PM HO scenario and is presented in Figure 4A-F. The analysis predicts that 90% is the maximum R_{HOS} for β_{ISD} of 500 m when configured with the HCP values which trigger early HO. The R_{HOS} decreases with a further increase in β_{ISD} and it is 24.28% for β_{ISD} = 700 m and 10.9% for β_{ISD} = 1100 m.

As mentioned before, the reasons are the transmit power disparity and the uplink/downlink coverage imbalance. An extension of this analysis is made for illustrating the influence of $\mathcal{E}$ on R_{HOS} and is shown in Figure 5A-E. It is inferred from the results that decrease in R_{HOS} is noted with an increase in offloading and vice versa. A maximum of 24% of R_{HOS} is

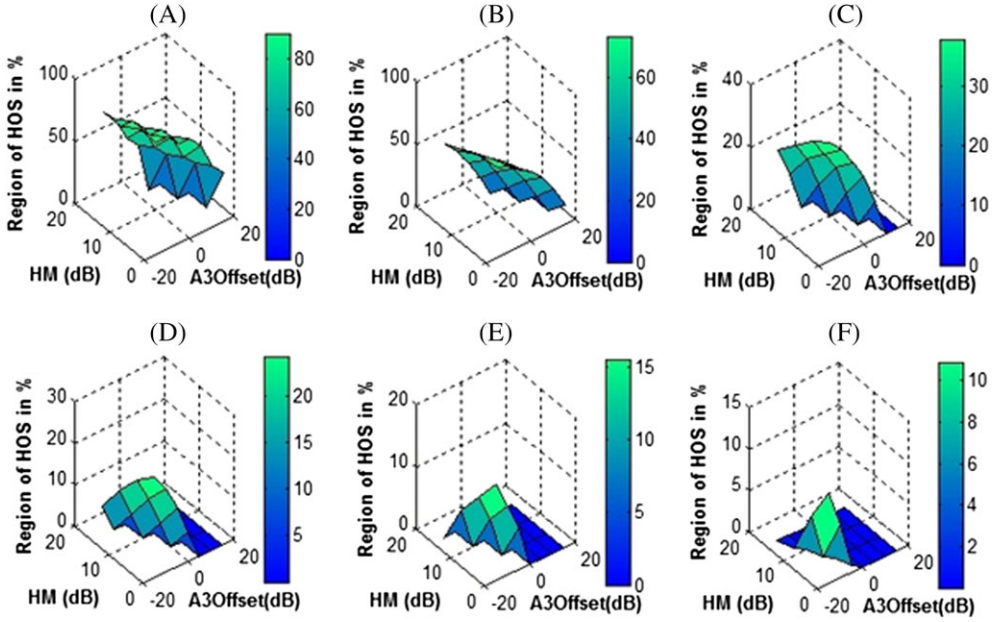

FIGURE 4 Sensitivity analysis of β_{ISD}. A, Pico-Macro ISD = 100m; B, Pico-Macro ISD = 300m; C, Pico-Macro ISD = 500m; D, Pico-Macro ISD = 700m; E, Pico-Macro ISD = 900m; Pico-Macro ISD = 1100m

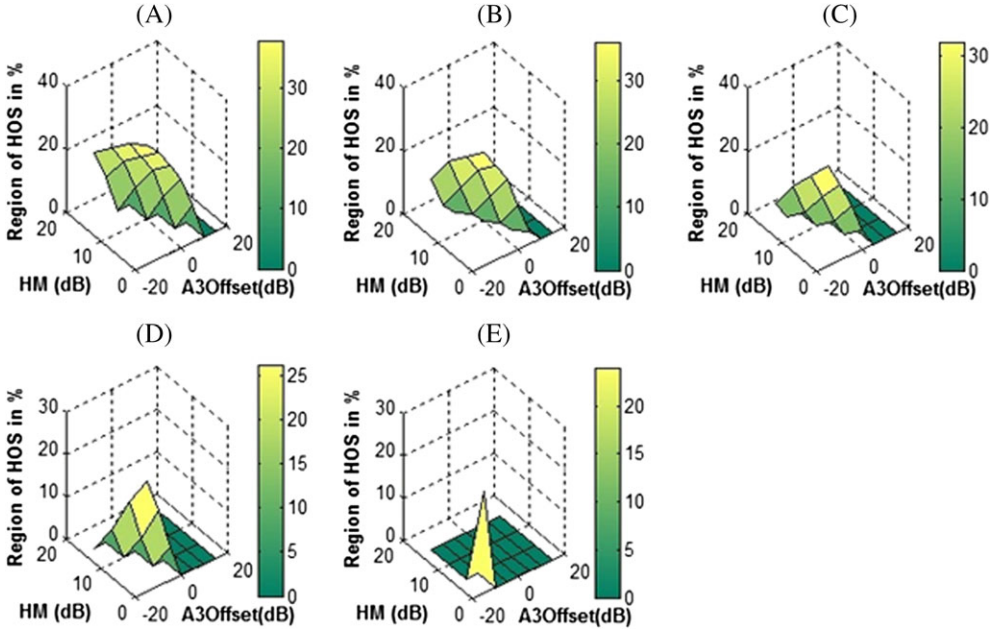

FIGURE 5 Sensitivity analysis of $\mathcal{E}$. A, CSO = 0 dB; B, CSO = 4 dB; C, CSO = 8 dB; D, CSO = 12 dB; E, CSO = 16 dB

achieved for maximum offloading, whereas it is 38% for null offloading. This is due to the fact that a larger value of $\mathcal{E}$ prevents the HO triggering process and makes the UE remain attached to S_{eNodeB} itself when compared to the configuration of null offloading. However, this larger value of $\mathcal{E}$ makes the target cell best in the uplink than in the downlink connection as long as the UE is in the coverage imbalance region.[26] The results reveal that the combinations of HCP values which trigger the HO early result in an increased R_{HOS} and the metrics β_{ISD} and $\mathcal{E}$ can be used to model their dependence on HO performance.

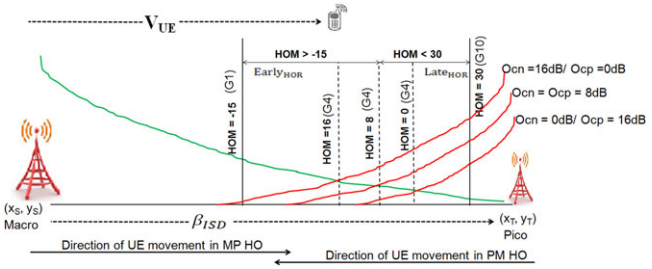

FIGURE 6 Early and late handover (HO) regions in macro-pico (MP) and pico-macro (PM) HO scenarios. UE, user equipment

4.3 | Formulation of HCP combination groups

As presented earlier, the HOS is verified for all the HCP value combinations (=140) in all the 30 simulation scenario sets considered. Among the 140 combinations, the occurrence of A3 event at the same point was seen during the analysis for certain HCP value combinations. Those HCP value combinations are grouped together and it results in 10 such groups from G1 to G10 for each value of CSO as mentioned in Table 4.

The CSO represents either Oc_n or Oc_p depending on the HO scenario considered and is configured depending on the need of offloading benefit required by the operator. From here onwards, in the analysis and the model development procedure, the discussion involves a number of groups rather than individual combinations of HCP values. A pictorial representation of the groups and their trigger points is shown in Figure 6. It can be seen that the early HO ($Early_{HOR}$) occurs for groups G1 to G3, whereas groups G5 to G10 trigger the late HO ($Late_{HOR}$) irrespective of the offloading benefit considered.

In addition, group G4 triggers exactly at the intersection point. In the $Early_{HOR}$, the sum value of HM and A3Off, ie, HOM is negative, and for $Late_{HOR}$, it is positive. When HOM is zero, the HO triggers exactly in the middle of ISD. In addition, the distance at which the groups trigger the HO varies with respect to the value of CSO. With larger Oc_n, HO triggers early compared to the smaller value of Oc_n in MP HO scenario while it is converse with the PM HO scenario, where Oc_p of 0 dB triggers the HO early and vice versa. The early trigger groups (G1-G3) reduce the duration of association with S_{eNodeB}, as the HO is triggered well before the boundary and vice versa with the late trigger groups (G5-G10).

4.4 | Impact of ISD and offloading benefits on HO success for both MP and PM HO scenario

The number of groups which trigger the HO and resulted in HOS is identified for both the characteristics of ISD and offloading benefits. These 10 groups are configured for each scenario to study the impact on MP HO performance for $\alpha = 10°$ as mentioned previously. Figure 7 represents the impact of ISD and offloading in the MP HO scenario. The inferences are (1) as β_{ISD} increases, γ decreases irrespective of the offloading benefit and (2) the number of groups which results in HOS increases with increase in offloading. The conclusion is that with an increase in β_{ISD}, initiation of the HO procedure should be made earlier by configuring early trigger groups. This is because as β_{ISD} increases, the region of overlapping decreases between S_{eNodeB} and T_{eNodeB}, which in turn increases the probability of occurrence of RLF before the successful completion of HO procedure.

The outcome of a similar kind is observed with respect to β_{ISD} in the PM HO scenario analysis and is presented in Figure 8. However, the inverse reaction is observed with respect to ε that the number of groups which results in HOS decreases as the offloading increases. This is because the larger bias of offloading delays the HO initiation procedure making S_{eNodeB} stronger with respect to T_{eNodeB}. Hence, only the early trigger groups result in HOS compared to late trigger groups. In both the cases (MP/PM HO scenario), degradation in the overall HO performance is observed when HCP is configured irrespective of β_{ISD} and ε. Thus, a regression-based prediction model is developed, utilizing the dependency of β_{ISD} and ε on HCP configuration and is presented in the next section.

4.5 | Analysis on region of HOS with respect to groups

The analysis has been further extended to visualize the impact of each configured group on R_{HOS}. Figures 9 to 12 represent the impact of β_{ISD} on R_{HOS} for the configured groups in the MP and PM HO scenarios with null and full offloading.

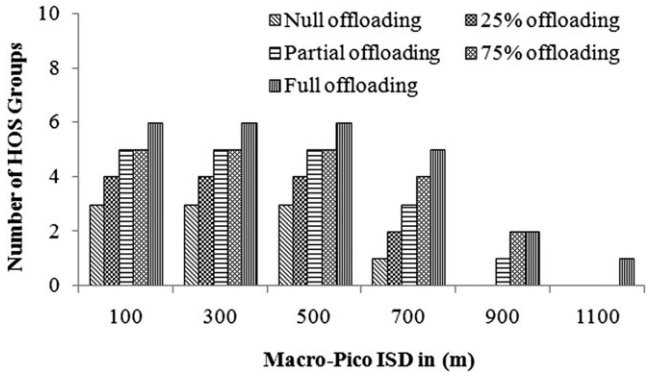

FIGURE 7 Impact of intersite distance (ISD) and offloading analysis for macro-pico (MP) handover (10°)

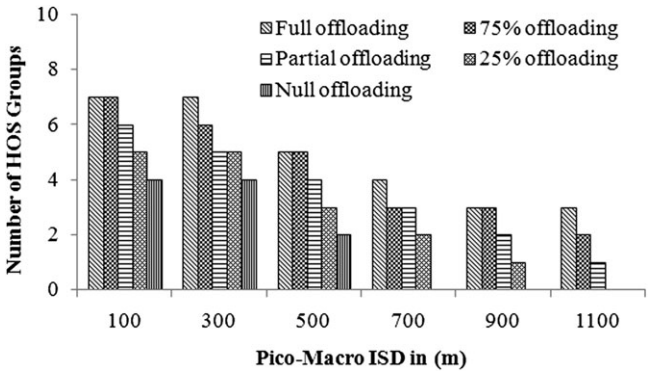

FIGURE 8 Impact of intersite distance (ISD) and offloading analysis for pico-macro (PM) handover (50°)

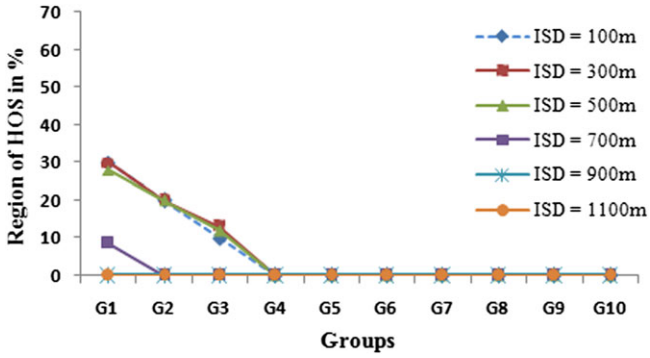

FIGURE 9 Null offloading in macro-pico handover scenario. ISD, intersite distance

Figure 9 shows R_{HOS} (in percentage) as almost similar with variation between 30% and 10% from G1 to G3 in the MP HO scenario when β_{ISD} is varied from 100 to 500 m for null offloading. As β_{ISD} increases, the HOS region decreases further to 9% (G1) for β_{ISD} of 700 m and no group results in HOS for β_{ISD} from 900 to 1100 m.

Figure 10 shows variation in R_{HOS} in the case of full offloading as follows: (1) from 60% to 20% (G1-G6) for β_{ISD} of 100 m, (2) from 52% to 12% (G1-G6) for β_{ISD} of 300 m, (3) from 53% to 12% (G1-G6) for β_{ISD} of 500 m, (4) from 35% to 10% (G1-G4) for β_{ISD} of 700 m, (5) from 18% to 8% (G1 and G2) for β_{ISD} of 900 m, and (6) 5% (G1) for β_{ISD} of 1100 m in the MP HO scenario. While in the PM HO scenario, R_{HOS} varies as follows in the case of null offloading: (1) from 90% to 40% (G1-G7) for β_{ISD} of 100 m, (2) from 75% to 18% (G1-G7) for β_{ISD} of 300 m, (3) from 39% to 10% (G1-G5) for β_{ISD} of 500 m, (4) from

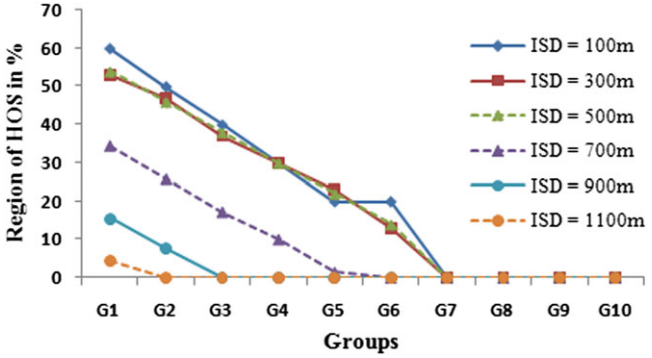

FIGURE 10 Full offloading in macro-pico handover scenario. ISD, intersite distance

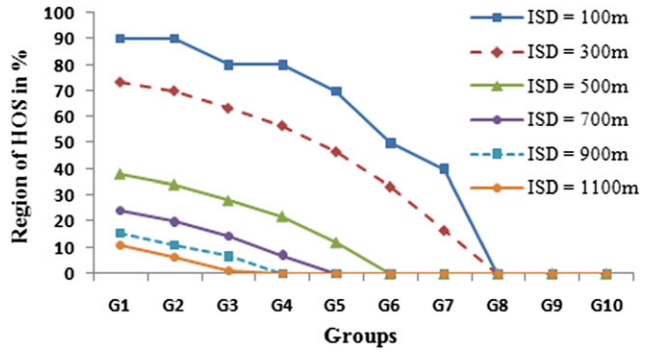

FIGURE 11 No offloading in pico-macro handover scenario. ISD, intersite distance

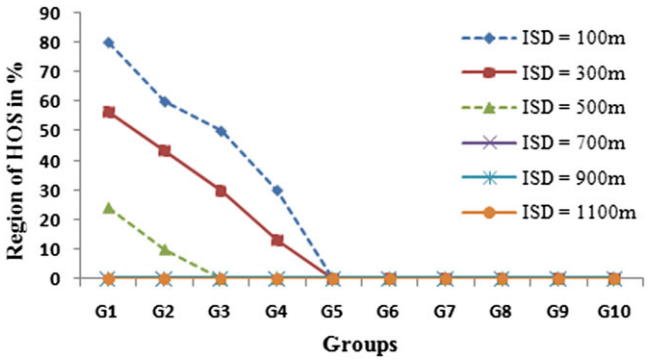

FIGURE 12 Full offloading in pico-macro handover scenario. ISD, intersite distance

25% to 8% (G1-G4) for β_{ISD} of 700 m, (5) from 18% to 8% (G1-G3) for β_{ISD} of 900 m, and (6) from 10% to7% (G1 and G2) for β_{ISD} of 1100 m as represented in Figure 10.

Figure 12 shows R_{HOS} variation in the case of full offloading for the PM HO scenario: from (1) 80% to 30% (G1-G4) for β_{ISD} of 100 m, (2) from 68% to 12% (G1-G4) for β_{ISD} of 300 m, (3) from 25% to 10% (G1 and G2) for β_{ISD} of 500 m, and (4) no region makes HOS for β_{ISD} of 700 to 1100 m.

The conclusion from the above analysis is that the same HCP group results in different R_{HOS} with respect to $\mathcal{E}$ and β_{ISD}. This is because, in the MP HO scenario, the higher offloading increases, the preference of HO at the early stage thereby R_{HOS} increases and vice versa, whereas in the PM HO scenario, the higher offloading delays, the HO decreases R_{HOS} and vice versa. Similarly, the overlapping region decreases with increase in β_{ISD} and vice versa in both MP and PM HO scenarios. In general, early triggering results in larger R_{HOS}, whereas late triggering decreases R_{HOS}.

From the above two analyses presented in Sections 4.4 and 4.5, the dependency of the factors $\mathcal{E}$ and β_{ISD} on HO performance improvement in terms of both the performance metrics γ and R_{HOS} was formulated as in Equation (17) and Equation (18). Both the performance metrics are directly proportional to $\mathcal{E}$ and inversely proportional to β_{ISD} as in

Equation (17) for MP HO scenario. Meanwhile, they are inversely proportional to both $\mathcal{E}$ and β_{ISD} in PM HO scenario as in Equation (18).

$$\textit{MP HO Scenario:} \quad (\gamma, R_{HOS}) \ \alpha \ \frac{\varepsilon}{\beta_{ISD}} \tag{17}$$

$$\textit{PM HO Scenario:} \quad (\gamma, R_{HOS}) \ \alpha \ \frac{1}{(\varepsilon, \beta_{ISD})} \tag{18}$$

The dependency in terms of a number of HOS groups is modeled as a regression model,[22] which identifies the HCP to be configured for the corresponding scenario.

4.6 | Model formulation

The results presented here emphasize the fact that the configuration of control parameters to trigger a successful HO should be based on the factors that include offloading benefits and the ISD. The prediction accuracy of the model is validated on the basis of the GoF metrics.[23] The better the "GoF" statistics, the higher the prediction accuracy of the model will be. The degree of the two factors controls the prediction accuracy. Hence, the regression models with the same and different degrees were developed to study their impact on prediction accuracy. They are discussed below.

Table 5 and Table 6 present the GoF statistics for the MP and PM HO scenarios with different possible combinations of polynomial degree. It is observed that the prediction accuracy increases as the degree of the model increases. However, the amount of computation gets increased with higher degree polynomial as (N + 1) terms are added to each polynomial model of degree N. For the polynomial P44, the prediction accuracy of 99.29% is achieved and is 0.29% lesser compared

TABLE 5 GoF metrics for different degrees (MP HO)

Polynomial (P′pq′)	SSE	RS	ARS	RMSE
P55 (*p* = 5 and q = 5)	1.466	0.99	0.9676	0.4036
P44 (p = 4 and q = 4)	1.03	0.9929	0.9863	0.262
P33 (*p* = 3 and q = 3)	4.128	0.9717	0.959	0.4543
P22 (*p* = 2 and q = 2)	10.77	0.9262	0.9108	0.6698
P11 (p = 1 and q = 1)	21.12	0.8552	0.8445	0.8844
P15 (p = 1 and q = 5)	2.234	0.9847	0.9766	0.3429
P14 (p = 1 and q = 4)	2.543	0.9826	0.9759	0.348
P13 (p = 1 and q = 3)	5.282	0.9638	0.9543	0.4792
P12 (p = 1 and q = 2)	10.87	0.9254	0.9135	0.6595
P51 (p = 5 and q = 1)	16.65	0.8858	0.8257	0.9363
P41 (p = 4 and q = 1)	17.72	0.8785	0.8323	0.9186
P31 (p = 3 and q = 1)	18.01	0.8765	0.8443	0.8849
P21 (p = 2 and q = 1)	19.06	0.8694	0.8485	0.8731

TABLE 6 GoF metrics for different degrees (PM HO)

Polynomial (P′pq′)	SSE	RS	ARS	RMSE
P55 (p = 5 and q = 5)	3.056	0.9748	0.9189	0.5827
P44 (p = 4 and q = 4)	1.685	0.9861	0.9732	0.3351
P33 (p = 3 and q = 3)	2.956	0.9757	0.9647	0.3844
P22 (p = 2 and q = 2)	4.366	0.9641	0.9566	0.4265
P11 (p = 1 and q = 1)	4.674	0.9615	0.9587	0.4161
P15 (p = 1 and q = 5)	2.21	0.9818	0.9722	0.341
P14 (p = 1 and q = 4)	2.388	0.9803	0.9728	0.3372
P13 (p = 1 and q = 3)	3.484	0.9713	0.9638	0.3892
P12 (p = 1 and q = 2)	4.413	0.9637	0.9579	0.4202
P51 (p = 5 and q = 1)	6.142	0.9494	0.9228	0.5686
P41 (p = 4 and q = 1)	4.051	0.9667	0.9539	0.4392
P31 (p = 3 and q = 1)	4.123	0.9661	0.9572	0.4234
P21 (p = 2 and q = 1)	4.604	0.9621	0.956	0.4291

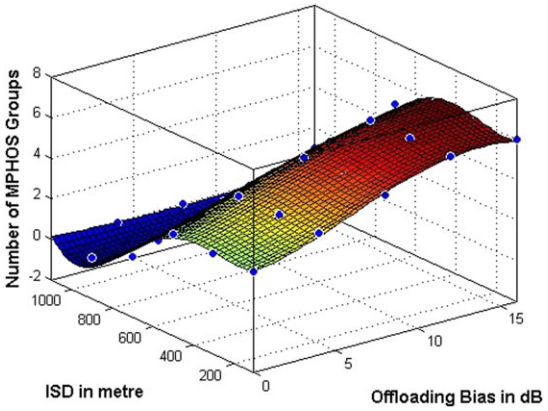

FIGURE 13 Surface model of the P44 of macro-pico (MP) handover scenario. ISD, intersite distance

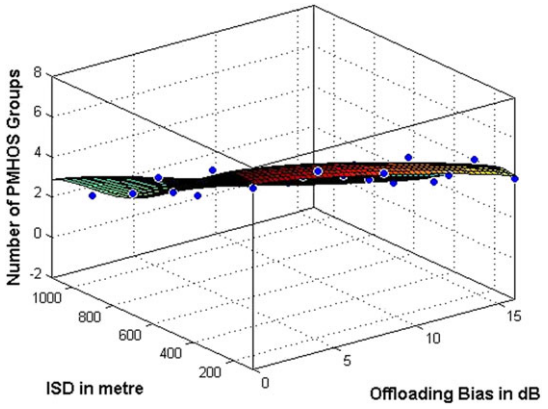

FIGURE 14 Surface model of the P44 of pico-macro (PM) handover scenario. ISD, intersite distance

to P55 while it is 0.82% and 2.12% higher when compared to P15 and P33. With respect to all other metrics such as SSE, adjusted R-square, and RMSE, the P44 model achieves the best result.

Similarly, the increase in prediction accuracy is observed up to P44 from Table 6, but it started to decrease for the next higher order degree of five. For the polynomial P44, the prediction accuracy of 98.61% is achieved which is 1.13% lesser compared to P55 and 0.43% and 1.04% higher when compared to P15 and P33. Hence, for both the MP and PM HO scenarios, the P44 model is confined as it presents the higher prediction accuracy to identify the number of HCP groups that can be configured with respect to β_{ISD} and $\mathcal{E}$. Figures 13 and 14 represent the obtained surface polynomial of the models with the same degree for the MP and PM HO scenarios.

The results show that, for both the HO scenario, the polynomial of higher degree $\mathrm{p} = q = 4$ (P44) fits the data more perfectly than the polynomial of other degrees $\mathrm{p} = \mathrm{q} = 1$(P11), $\mathrm{p} = 1$ and $\mathrm{q} = 4$ (P14) and $\mathrm{p} = 4$ and $\mathrm{q} = 1$ (P41). The independent variable in the polynomial with higher degree fits more perfectly than the independent variable with a lower degree. Equations 19 and 20 represent the P44 polynomial model of MP and PM HO scenarios.

$$\begin{aligned} \gamma_{44} = \mathrm{f}(\mathcal{E}, \beta_{\mathrm{ISD}}) = {} & \varphi_1 + \varphi_2\,\mathcal{E} + \varphi_3\,\beta_{\mathrm{ISD}} + \varphi_4\mathcal{E}^2 + \varphi_5\,\mathcal{E}\beta_{\mathrm{ISD}} \\ & + \varphi_6\beta_{\mathrm{ISD}}^2 + \varphi_7\mathcal{E}^3 + \varphi_8\mathcal{E}^2\,\beta_{\mathrm{ISD}} + \varphi_9\,\mathcal{E}\beta_{\mathrm{ISD}}^2 + \varphi_{10}\beta_{\mathrm{ISD}}^3 \\ & + \varphi_{11}\mathcal{E}^4 + \varphi_{12}\mathcal{E}^3\beta_{\mathrm{ISD}} + \varphi_{13}\mathcal{E}^2\beta_{\mathrm{ISD}}^2 + \varphi_{14}\,\mathcal{E}\beta_{\mathrm{ISD}}^3 + \varphi_{15}\beta_{\mathrm{ISD}}^4 \end{aligned} \tag{19}$$

The corresponding value of the polynomial coefficients with 95% confidence bounds is $\varphi_1 = 3.812$, $\varphi_2 = 0.03305$, $\varphi_3 = -0.01267$, $\varphi_4 = 0.05518$, $\varphi_5 = 0.0002911$, $\varphi_6 = 5.938\mathrm{e}{-05}$, $\varphi_7 = -0.003733$, $\varphi_8 = -6.425\mathrm{e}{-05}$, $\varphi_9 = 2.078\mathrm{e}{-07}$,

$\varphi_{10} = -1.007e{-}07$, $\varphi_{11} = 5.425e{-}05$, $\varphi_{12} = 2.604e{-}06$, $\varphi_{13} = 1.794e{-}08$, $\varphi_{14} = -4.919e{-}10$, and $\varphi_{15} = 4.948e{-}11$.

$$\begin{aligned} \Upsilon_{44} = f(\mathcal{E}, \beta_{ISD}) = {} & \varphi_1 + \varphi_2\,\mathcal{E} + \varphi_3\,\beta_{ISD} + \varphi_4\mathcal{E}^2 \\ & + \varphi_5\,\mathcal{E}\beta_{ISD} + \varphi_6\beta_{ISD}^2 + \varphi_7\mathcal{E}^3 + \varphi_8\mathcal{E}^2\,\beta_{ISD} + \varphi_9\,\mathcal{E}\beta_{ISD}^2 \\ & + \varphi_{10}\beta_{ISD}^3 + \varphi_{11}\mathcal{E}^4 + \varphi_{12}\mathcal{E}^3\beta_{ISD} + \varphi_{13}\mathcal{E}^2\beta_{ISD}^2 + \varphi_{14}\,\mathcal{E}\beta_{ISD}^3 + \varphi_{15}\beta_{ISD}^4 \end{aligned} \tag{20}$$

The corresponding value of the polynomial coefficients with 95% confidence bounds is $\varphi_1 = 6.125$, $\varphi_2 = -0.1252$, $\varphi_3 = 0.01732$, $\varphi_4 = -0.008411$, $\varphi_5 = 0.000245$, $\varphi_6 = -7.305e{-}05$, $\varphi_7 = 0.0007378$, $\varphi_8 = -4.608e{-}05$, $\varphi_9 = 1.44e{-}07$, $\varphi_{10} = 8.403e{-}08$, $\varphi_{11} = -2.713e{-}05$, $\varphi_{12} = 1.302e{-}06$, $\varphi_{13} = 2.192e{-}08$, $\varphi_{14} = -3.183e{-}10$, and $\varphi_{15} = -3.125e{-}11$.

Furthermore, a learning approach can be designed to confine the model output as it defines the number of HOS groups.

5 | CONCLUSION AND FUTURE WORK

In order to improve the success rate of HO procedure, regression-based prediction model for HCP configuration has been developed utilizing the dependent factors identified from the preliminary analysis. The dependent factors identified are ISD and offloading benefit. The regression models were developed for different degrees to improve prediction accuracy. The P44 model presents the highest accuracy for both the MP and PM HO scenarios when compared to the other lower and higher order models.

The advantage of the presented method is that it does not rely on expert knowledge and also long-term stability can be ensured as it depends on fixed characteristics. The proposed work can be implemented at the base station site by the network service provider for reducing the search space in HCP configuration thereby achieve improved performance of LTE-A network. However, an efficient reinforcement learning method could be developed in future work to arrive at the optimal value of HCP by incorporating the various conclusions arrived in the works of Saraswathi Priyadharshini and Bhuvaneswari.[16,17]The study has to be extended considering the user service type as suggested in the work of Al-Turjman et al.[27]

ORCID

A. Saraswathi Priyadharshini https://orcid.org/0000-0001-5010-5968

REFERENCES

1. Calabuig D, Barmpounakis S, Gimenez S, et al. Resource and mobility management in the network layer of 5G cellular ultra-dense networks. *IEEE Commun Mag*. 2017;55(6):162-169.
2. 3GPP. http://www.3gpp.org
3. Cotanis I, Hedlund A. HetNets: Opportunities and Challenges. White Paper-An ASCOM Network Testing. 2013.
4. Parkvall S, Furuskar A, Dahlman E. Evolution of LTE toward IMT-advanced. *IEEE Commun Mag*. 2011;49(2):84-91.
5. Korhonen J. *Introduction to 3G Mobile Communications*. 2nd ed. Norwood, MA: Artech House; 2003. *Artech House Mobile Communications Series*.
6. 3GPP. Universal mobile telecommunications system (UMTS); LTE; non-access-stratum (NAS) protocol for evolved packet system (EPS). (Release 13) TS 24.301, V13.4.0, 3rd Generation Partnership Project (3GPP). March 2016.
7. 3GPP. LTE; general packet radio service (GPRS) enhancements for evolved universal terrestrial radio access network (E-UTRAN). (Release 13) TS 23.401, V13.5.0, 3rd Generation Partnership Project (3GPP). March 2016.
8. 3GPP. LTE; telecommunication management; performance management (PM); performance measurements evolved universal terrestrial radio access network (E-UTRAN). (Release 13) TS 32.425, V13.3.0, 3rd Generation Partnership Project (3GPP). March 2016.
9. 3GPP. Evolved universal terrestrial radio access (E-UTRA); radio resource control (RRC); protocol specification. (Release 13) TS 36.331, V13.1.0, 3rd Generation Partnership Project (3GPP). April 2016.
10. Al-Turjman FM. Modelling green femtocells in smart-grids. In: *Smart Things and Femtocells*. Boca Raton, FL: Springer Mobile Network and Applications; 2018:940-955.
11. Lee Y, Shin B, Lim J, Hong D. Effects of time-to-trigger parameter on handover performance in SON-based LTE systems. Paper presented at: IEEE-16th Asia-Pacific Conference on Communications (APCC); 2010; Auckland, New Zealand.
12. Barbera S, Michaelsen PH, Saily M, Pedersen K. Mobility performance of LTE co-channel deployment of macro and pico cells. Paper presented at: IEEE-Wireless Communications and Networking Conference (WCNC); April 2012; Shanghai, China.
13. Lim J, Hong D. Mobility and handover management for heterogeneous networks in LTE-advanced. *J Wirel Pers Commun*. 2013;72(4):2901-2912.

14. Mehta M, Akhtar N, Karandikar A. Impact of handover parameters on mobility performance in LTE HetNets. Paper presented at: Twenty-First National Conference on Communications (NCC); March 2015; Mumbai, India.
15. Kollias G, Adelantado F, Verikoukis C. The impact of inter-site distance and time-to-trigger on handover performance in LTE-A HetNets. Paper presented at: IEEE-International Conference on Communications (ICC); June 2015; London, UK.
16. Saraswathi Priyadharshini A, Bhuvaneswari PTV. Handover control parameter configuration in LTE-a network. Paper presented at: IEEE-International Conference on Innovations in Electronics, Signal Processing and Communication (IESC); April 2017; Shillong, India.
17. Saraswathi Priyadharshini A, Bhuvaneswari PTV. Interdependency analysis of angle of UE movement and inter-site-distance on configuration of handover control parameter in LTE-a HetNets. Paper presented at: IEEE-International Conference on Signal Processing, Communication and Networking (ICSCN); March 2017; Chennai, India.
18. Munoz P, Barco R, de la Bandera I. On the potential of handover parameter optimization for self-organizing networks. *IEEE Trans Veh Technol*. 2013;62(5):1895-1905.
19. Mwanje SS, Mitschele-Thiel A. Distributed cooperative Q-learning for mobility-sensitive handover optimization in LTE SON. Paper presented at: IEEE Symposium on Computers and Communication (ISCC); June 2014; Funchal, Portugal.
20. Hegazy RD, Nasr OA. A user behavior based handover optimization algorithm for LTE networks. Paper presented at: IEEE Wireless Communications and Networking Conference (WCNC); 2015; New Orleans, LA.
21. Becvar Z, Mach P. Adaptive hysteresis margin for handover in femtocell networks. Paper presented at: IEEE Computer Society-Sixth International Conference on Wireless and Mobile Communications; 2010; Valencia, Spain.
22. Saraswathi Priyadharshini A, Bhuvaneswari PTV. Regression model for handover control parameter configuration in LTE-a networks. *Comput Electr Eng*. 2018;72:877-893.
23. Goodness-of-Fit Statistics. http://web.maths.unsw.edu.au/~adelle/Garvan/Assays/GoodnessOfFit.html
24. 3GPP. Technical specification group radio access network; evolved universal terrestrial radio access (E-UTRA); mobility enhancements in heterogeneous networks. (Release 11) TR 36.839, V11.1.0 (2012-12), 3rd Generation Partnership Project (3GPP). December 2012.
25. 3GPP. Technical specification group radio access network; evolved universal terrestrial radio access (E-UTRA); further advancements for E-UTRA physical layer aspects. (Release 9) TR 36.814, V9.0.0, 3rd Generation Partnership Project (3GPP). March 2010.
26. Giluka MK, Khan MSA, Krishna GM, Atif TA, Sathya V, Tamma BR. On handovers in uplink/downlink decoupled LTE HetNets. Paper presented at: IEEE Wireless Communications and Networking Conference (WCNC); 2016; Doha, Qatar.
27. Al-Turjman F, Ever E, Zahmatkesh H. Green femtocells in the IoT era: traffic modelling and challenges—an overview. *IEEE Netw Mag*. 2017;31(6):48-55.

How to cite this article: Saraswathi Priyadharshini A, Bhuvaneswari PTV. Regression model for seamless mobility in LTE-A HetNets. *Trans Emerging Tel Tech*. 2019;e3570. https://doi.org/10.1002/ett.3570